


Promotion of bone cancer pain development by decorin is accompanied by modification of excitatory synaptic molecules in the spinal cord

Molecular Pain
Volume 15: 1–11
© The Author(s) 2019
Article reuse guidelines:
sagepub.com/journals-permissions
DOI: 10.1177/1744806919864253
journals.sagepub.com/home/mpx



Huan Wang^{1,*} , Xiaohui Li^{1,*}, Xianqiao Xie¹, Haiwen Zhao¹, Yan Gao², Yang Li¹, Xueqin Xu¹, Xiaofei Zhang¹, Changbin Ke¹, and Juying Liu¹

Abstract

Bone cancer pain is refractory to currently available clinical treatment owing to its complicated underlying mechanisms. Studies found that extracellular matrix molecules can participate in the regulation of chronic pain. Decorin is one of the most abundant extracellular matrix molecules, and the present study evaluated the effect of decorin on the development of bone cancer pain. We found that decorin was upregulated in the L4–L6 spinal dorsal horn of the bone cancer pain rats. Spinal microinjection of a decorin-targeting RNAi lentivirus alleviated bone cancer pain-induced mechanical allodynia and reduced the expression of pGluR1-Ser831 in the bone cancer pain rats. Meanwhile, decorin knockdown impaired the excitatory synaptogenesis in cultured neurons and prevented the clustering and insertion of pGluR1-Ser831 into postsynaptic membranes. Taken together, the results of our study suggested that decorin contributes to the development of bone cancer pain possibly by regulating the activity of excitatory synaptic molecules in the spinal cord. Our findings provide a better understanding of the function of decorin as a possible therapeutic target for alleviating bone cancer pain.

Keywords

Decorin, bone cancer pain, AMPA receptor, synapse

Date Received: 3 June 2018; revised: 16 June 2019; accepted: 18 June 2019

Introduction

Pain is one of the most common symptoms for cancer patients, and bone pain is the most common type of cancer-induced pain.¹ Bone cancer pain (BCP) is a complex and intractable pathologic condition that severely affects the patient's quality of life. Typical characteristics of BCP are allodynia, hyperalgesia, spontaneous ongoing pain, and incident breakthrough pain, which are different from inflammatory pain and neuropathic pain.² Currently, the underlying mechanism of the BCP remains poorly understood.

In the pain-sensing pathway, primary sensory neurons located in the dorsal root ganglion transduce and convey somatic and visceral nonnociceptive or nociceptive stimuli to the spinal dorsal horn and brain stem,³ and the signal transduction between neurons in the pathway is primarily accomplished through synapses. Central sensitization of the spinal cord induced by

synaptic plasticity of glutamatergic transmission plays an important role in the induction and maintenance of the BCP.^{4–6} Glutamate serves as the primary excitatory neurotransmitter between glutamatergic transmissions in the somatosensory nociceptive pathway in which it can

¹Department of Anesthesiology, Institute of Anesthesiology & Pain, Taihe Hospital, Hubei University of Medicine, Shiyan, Hubei, China

²Department of PET Center, Taihe Hospital, Hubei University of Medicine, Shiyan, Hubei, China

*The first two authors contributed equally to this work.

Corresponding Authors:

Changbin Ke, Department of Anesthesiology, Institute of Anesthesiology & Pain, Taihe Hospital, Hubei University of Medicine, Shiyan, 442000, China. Email: changbinke-iap@taihehospital.com

Juying Liu, Department of Anesthesiology, Institute of Anesthesiology & Pain, Taihe Hospital, Hubei University of Medicine, Shiyan, 442000, China. Email: Liu6119@163.com



activate both ionotropic and metabotropic receptors.^{7–9} A previous study¹⁰ has demonstrated that both N-methyl-D-aspartate and metabotropic glutamate (mGlu) receptors participate in the development of the BCP, while the roles of α -amino-3-hydroxy-5-methyl-4-isoxazolepropionic acid receptors (AMPA) are unclear.

Extracellular matrix (ECM) molecules, which include proteoglycans, fibrous proteins, and collagen, participate in various cell biological processes, such as proliferation,¹¹ migration,¹² morphological, and biochemical differentiation, as well as synaptogenesis and synaptic activity in the nervous system.¹³ An increasing number of studies have showed that ECM plays an important role in the synaptic plasticity of the nervous system.^{13–15} Decorin, a member of the small leucine-rich proteoglycans family, is an important component of ECM capable of inhibiting the biological effect of transforming growth factor- β (TGF- β) and epidermal growth factor receptor tyrosine kinase¹⁷ and has anti-inflammatory and antifibrotic functions. In the nervous system, decorin^{18,19} has unique advantages in promoting the extension and branching of injured axons by suppressing the synthesis of axon growth inhibitors, the levels of axon growth inhibitory chondroitin sulfate proteoglycans and the formation of fibrotic scar. However, the role of decorin in synaptic plasticity is unclear.

Semaphorins, a large family of secreted and membrane-bound glycoproteins, function in axon guidance, dendritic spine morphology and maturation, and synapse formation in the developing and adult nervous system.²⁰ Sema3a was the first semaphorin to be identified in a vertebrate and induces the retraction and collapse of structure on the axonal growth cone. Our previous study demonstrated that the downregulation of sema3a in the spinal dorsal horn contributed to the BCP in a rat model by decreasing the phosphorylation level of cofilin. Minor²¹ found that in addition to suppressing the levels of inhibitory chondroitin sulfate proteoglycans, decorin has the ability to reduce the messenger RNA and protein levels of sema3a in an injured central nervous system. However, the relationship between decorin and sema3a in BCP has not been reported.

In the present study, we first implanted carcinoma cells into the tibial plateau of rats to establish a model of BCP. *In vivo* and *in vitro* experiments were performed to examine the effects of decorin on the BCP and the relevant mechanisms.

Materials and methods

Animals

Female Sprague–Dawley (SD) rats weighing 80–120 g and 180–220 g provided by the Institute of Laboratory Animal Science, Hubei University of Medicine were

housed in private cages at room temperature (RT; 20°C) with a 12 h/12 h light/dark cycle and with food and water available *ad libitum*. The experimental procedures and protocols were approved by the Animal Care and Use Committee of Hubei University of Medicine (Hubei, China) and were in accordance with the guidelines for pain research on laboratory animals.²²

Preparation of Walker 256 cells

Walker 256 rat mammary gland carcinoma cells (0.5 ml , 6×10^7 cells/ml) were injected into the enterocoelia of female SD rats weighing 80–120 g. One week later, 10 ml ascitic fluid were drawn from the rat to extract and collect carcinoma cells. First, the cells were resuspended in phosphate-buffered solution (PBS) three times to remove red blood cells; then, the cells were counted to prepare for final fresh cell suspensions (5×10^7 cells/ml). For the sham group, the cells were prepared in the same concentrations and boiled for 30 min before the BCP model establishment.

BCP model

Walker 256 cells ($20 \mu\text{l}$, 5×10^7 cells/ml) were injected into the tibial plateau of SD rats weighing 180–220 g to establish the BCP model, the detailed procedures referenced to previous study.²³ Briefly, experimental rats were anesthetized with isoflurane (3% induction, 2% maintenance) and placed on an operating table in the supine position; afterward, the skin overlying the right tibial plateau of rats were sterilized with 75% v/v ethanol after being carefully shaved. After we drilled into the rats' tibial plateau with a 23-gauge needle, a $20\text{-}\mu\text{l}$ solution of tumor cells ($20 \mu\text{l}$, 5×10^7 cells/ml) or boiled tumor cells was slowly injected into the bone marrow cavity with a $25\text{-}\mu\text{l}$ glass microinjector. Following the carcinoma implantation, intraspinal microinjection surgery was performed on the rats.

Lentivirus construction and intraspinal microinjection

Lentiviral vectors with a green fluorescent protein (GFP) were used to stably knockdown the expression of decorin. The vectors GV493 (hU6-MCS-CBh-gcGFP) and decorin gene (GenBank accession number NM_029139) and vectors GV303 (pUbi-MCS-SV40-EGFP) and sema3a gene (NM_017310) were recombined by the Genechem Company (Genechem, Shanghai, China), and we named the two lentiviral vectors shdecorin and sema-LV, respectively. The same vector frameworks carrying no gene sequence were used as the negative control lentivirus, named shctrl and ctrl-LV, respectively. The viral titer of the lentivirus was 8.0×10^8 TU/ml.

The steps for the microinjection of lentivirus in the spinal cord were similar to those described in a previous study.²⁴ The experimental rats were anesthetized with isoflurane following carcinoma injection in the tibial plateau and placed on the operating table in prone position; the backs were shaved at the dorsal level, and a cutaneous incision (3 cm) was performed to expose the backbone. Then, the L4–L6 lumbar spinal cord was exposed by carefully removing the surrounding muscle and the L1 vertebrae. A glass capillary ($35 \pm 5 \mu\text{m}$ diameter) connected to a glass microinjector ($10 \mu\text{l}$) was used for lentivirus microinjection, and the needle was inserted 0.5 cm along the right side of the spinal dorsal horn midline at a depth of 0.4 cm to reach the dorsal horn; $5 \mu\text{l}$ (2.0×10^8 TU) of the viral suspension was injected into the rats at a rate of $0.5 \mu\text{l}/\text{min}$. Finally, the incision was dusted with penicillin powder, and the skin was sutured. The rats were put on a warm pad for anesthesia recovery and then transferred to separate cages for feeding.

Behavioral analysis

The behavioral of the rats was analyzed in a blinded manner between 08:00 a.m. and 11:00 a.m. in a quiet room. Mechanical allodynia of the rats were assessed using the paw withdrawal threshold (PWT) with a dynamic plantar esthesiometer (Ugo Basile, Comerio, Italy), an automated version of the von Frey hair test. Both measurements were carried out 0, 3, 5, 7, 10, 14, and 21 days after BCP surgery. The rats were placed individually on wire mesh platforms in transparent perspex box ($20 \text{ cm} \times 25 \text{ cm} \times 15 \text{ cm}$) and habituated for 30 min to allow acclimatization to the new environment. During each measurement, a straight metal filament (0.5 mm diameter) was raised until it touched the ipsilateral hind paw of the rats, and the force (g) was increased until the paw was withdrawn; the final force on the esthesiometer was the PWT of the rat. The ipsilateral hind paw of each rat was measured three times at an interval of 10 min, and the average of three values was used for data analysis.

Primary neuron culture and transfection

Primary cultures of cortical neurons were prepared from postnatal day 0 (P0) rat pups as previously described. First, the cortical tissues removed from the newborn rats were transferred into a sterile culture dish and washed with ice-cold PBS to remove the red blood cells. Next, the tissues were transferred to another culture dish containing Dulbecco's Modified Eagle Medium (DMEM)-F12 medium and then digested with 0.25% trypsin-EDTA in an incubator for 15 min. Serum was added to stop the trypsin digestion, and the neurons were dissociated by gently pipetting up and down.

Finally, the cell suspensions were filtered by a filter screen (200 μ) and centrifuged at 800 r/min for 5 min. The neurons were placed on poly-D-lysine-coated coverslips in 24-well plates at a final density of 3×10^4 cells and cultured in DMEM-F12 medium supplemented with 10% fetal bovine serum at 37°C and 5% CO_2 for 2 h. Two hours after plating, the medium was replaced with Neurobasal-A medium containing 2% B-27. The neuronal culture medium was refreshed every three days. At DIV 3, the neurons were infected with shctrl or shdecorin lentivirus at a multiplicity of infection of 20 for 12 h in DMEM-F12 medium; the neurons in the control group were treated with PBS only.

Immunofluorescence analysis

To analyze the immunofluorescence of the spinal cords, at 21 days after the BCP surgery, the rats were deeply anaesthetized with 10% chloral hydrate (0.1–0.3 ml/100 g, intraperitoneal injection) and transcardially perfused with 37°C PBS for 3 min, followed by ice-cold 4% paraformaldehyde for 90 min. The L4–L6 spinal cord was quickly removed from the rats, postfixed in 4% paraformaldehyde at 4°C for 2 h, and treated with a 30% sucrose solution in PBS for 48 h at 4°C . The spinal cord was embedded with O.C.T compound at -20°C and sectioned on a freezing microtome (Leica, Germany) at $25 \mu\text{m}$ in the transverse plane. After being washed with PBS three times, the slices were blocked with 5% normal donkey serum in PBS for 10 min at RT and incubated with primary antibodies overnight at 4°C . The slices were washed with PBS three times the next day and incubated with Alexa fluorescent-conjugated secondary antibodies in darkness for 40 min at 37°C . The slices were examined with a confocal laser microscope (Leica TCS SP8, Wetzlar, Germany).

For immunofluorescence imaging of the neurons, cultured neurons at DIV 12 were fixed in 4% paraformaldehyde for 15 min at RT and washed with PBS three times; then, the neurons were permeabilized with 0.5% Triton X-100 in PBS for 10 min and washed with 0.1% Tween in PBS (PBST) three times. Afterward, the neurons were blocked with 5% normal donkey serum in PBS for 30 min at RT and incubated with primary antibodies overnight at 4°C . After being washed with PBST three times, the neurons were incubated with secondary antibodies in darkness at 37°C for 1 h. After mounting with 50% glycerol, the stained glass slides were analyzed with a confocal laser microscope.

The primary antibodies were diluted and used at the following dilutions: rabbit antidecorin (1:100, ab175404, Abcam), goat antisynapsin I (1:50, sc-8295, Santa), rabbit anti-gluR1 (1:50, ab109450, Abcam), rabbit anti-P-gluR1 (1:50, A4352, Sigma), mouse antipostsynaptic density protein 95 (PSD95; 1:50, MABN68,

Millipore), rabbit anti-Bassoon (1:500, 141002, Synaptic System), guinea pig anti-MAP2 (1:800, 188004, Synaptic System), and mouse anti-VGlu2 (1:50, MAB5504, Millipore).

Based on previously described methods, image acquisition and quantitative analysis were performed in a blinded manner. For the quantification of the synapses, three dendrites per neuron were randomly selected, and the number of synaptic puncta (Bassoon, VGlu2, PSD95, GluR1 and P-GluR1) per 30 μm of dendrite length was measured using the Puncta Analyzer plugin in ImageJ software. A total of 20–35 neurons per condition were analyzed in at least three independent experiments. Cortical neurons expressing GFP were randomly selected, and the numbers of dendritic spines per 40 μm of the primary or secondary dendritic branch were counted manually to estimate the density; 10–20 images from three independent experiments per condition were performed and analyzed.

Real-time quantitative PCR analysis

For the real-time polymerase chain reaction (PCR) analysis, at 21 days after the BCP surgery, the rats were deeply anaesthetized with 10% chloral hydrate, and the L4–L6 spinal cord was quickly removed to an ice-chilled lysis buffer through laminectomy. Total RNA was extracted from the spinal cord using the Trizol reagent and reverse transcribed according to the manufacturer's instructions (Takara, Japan). The expression of the targeted genes was analyzed by quantitative real-time PCR on a SYBR Green qPCR Master Mix reagent system (Takara, Japan). The sequences of forward (F) and reverse (R) primers used are listed as follows: glyceraldehyde 3-phosphate dehydrogenase: F: 5'-AGGT CGGTGTGAACGGATTTG-3', R: 5'-TGTAGACCA TGTAGTTGAGG TCA-3'; decorin: F: 5'-CCTTCT GGCGCAAGTCTCTT-3', R: 5'-AACACTGCACCA CTCGGAGA-3'; sema3a: F: 5'-GGATTTTCATGGGA CGAGACTTTG-3', R: 5'-AGATGGGACTGATGAA TCTAGGA-3'; and Glur1: F: 5'-CAGC GACGGCAA TATGGAG-3', R: 5'-CCGGACCAAGGTTATGGT CAA-3'.

Western blot analysis

Twenty-one days after the BCP surgery, the rats were deeply anaesthetized with 10% chloral hydrate, and the L4–L6 spinal cord was removed and transferred quickly to ice-chilled radio-immunoprecipitation assay (RIPA) lysis buffer. The tissues were homogenized for 1 min and disintegrated on ice for 30 min, and the homogenates were centrifuged at 12,000 g for 15 min at 4°C to separate the total protein extract from the precipitate. The concentration of the total protein was measured

by the BCA protein assay kit. Western blot assay was performed similar to a previous study.²⁵

Statistical data analysis

All data were analyzed using SPSS 22.0 software, and results are shown as mean \pm standard error of the mean. One-way analysis of variance were performed to compare the differences between multiple groups, and *t* tests were performed in pairwise comparisons. Differences were considered statistically significant when $p < 0.05$. The sample sizes and significance are presented in the figure legends.

Results

The upregulation of decorin in ipsilateral spinal dorsal horn promoted BCP development

To detect whether decorin participated in the pathogenesis of BCP, we first examined the expression of decorin in the lumbar (L4–L6) spinal dorsal horn. The immunofluorescence staining of spinal cross sections showed that decorin was expressed in the spinal cord and increased in ipsilateral spinal cord, especially in the dorsal horn of the BCP but not in the contralateral side when compared with the sham rats (Figure 1(a)). To further investigate the role of decorin in BCP, recombinant RNAi lentivirus-targeting decorin (shdecorin) or the control lentivirus (shctrl) was microinjected into the ipsilateral dorsal horn of the BCP rats. Real-time PCR (Figure 1(b)) and western blot analysis (Figure 1(c)) showed that the mRNA and protein levels of decorin were significantly higher in the BCP group ($p < 0.05$) than in the sham group and were significantly downregulated by shdecorin ($p < 0.05$) but not by shctrl when compared with the BCP group.

The paw withdraw threshold (PWT) of the rats were measured to detect the effect of decorin on mechanical allodynia. First, the carcinoma cells were injected into the tibial plateau of the rats to establish the BCP model, and the lentivirus was microinjected into the ipsilateral dorsal horn on the same day as the carcinoma implantation surgery; we tested the PWT of rats' ipsilateral paws 0, 3, 5, 7, 10, 14, 17, and 21 days after surgery. There was no significant difference in basic PWT for all rats before surgery. From the seventh day, the PWT was significantly lower in rats from the BCP group than in rats from the sham group; meanwhile, treatment with shdecorin but not the shctrl prevented the reduction of PWT compared with the BCP rats ($p < 0.05$) (Figure 1(d)). Taken together, these results suggest that the upregulation of decorin promoted the development of BCP.

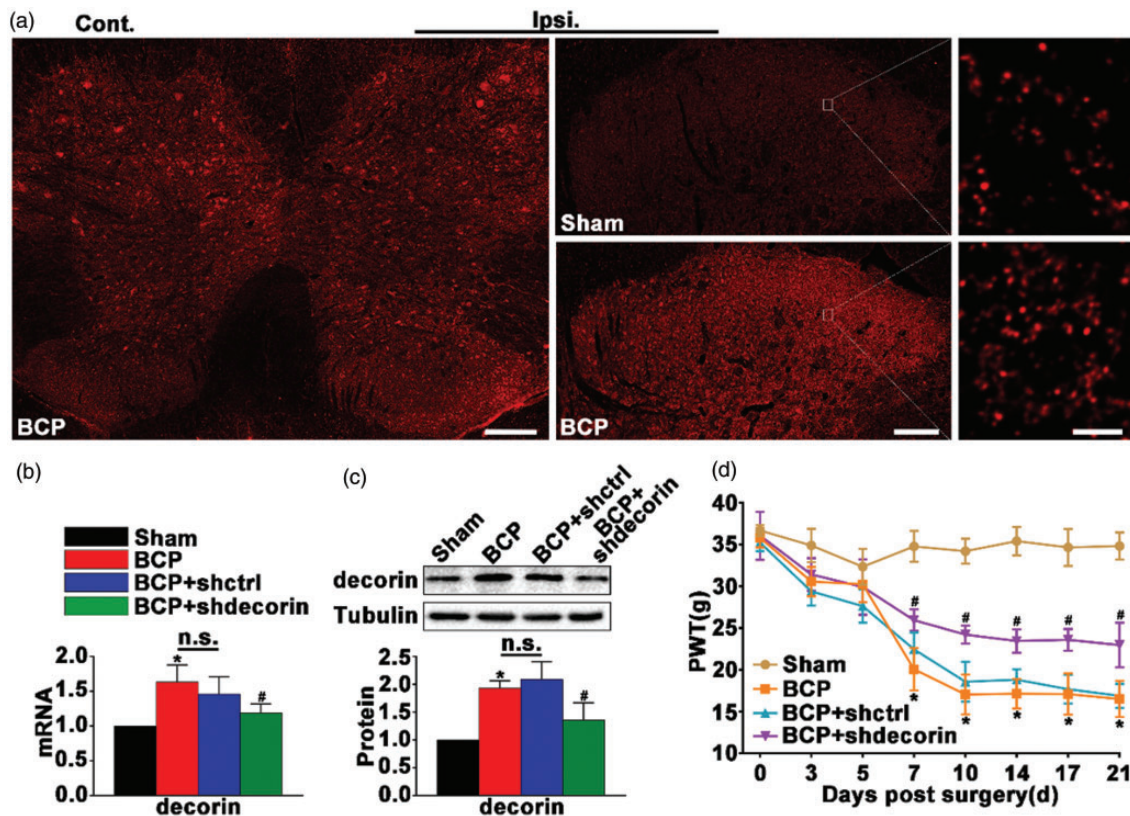


Figure 1. Upregulation of decorin in the ipsilateral spinal dorsal horn of carcinoma-implanted rats. (a) Immunofluorescence of decorin in transverse sections of the lumbar (L4–L6) spinal cord in sham and BCP rats. Spinal cord stainings showed that decorin expression was increased in the ipsilateral spinal cord of the BCP rats, especially in the dorsal horn compared with either the contralateral side or the sham rats. The right images show the high-magnification images of the ipsilateral dorsal horn in the sham and BCP rats. Scale bar: left 200 μm , middle 100 μm , and right 4 μm . (b, c) The knockdown efficiency of decorin in the lumbar (L4–L6) spinal cord of the sham, BCP, BCP+shctrl, and BCP+shdecorin rats 21-day postsurgery was confirmed by real-time polymerase chain reaction and western blotting. BCP rats: BCP rats; BCP+shctrl rats: BCP rats treated with the control lentivirus; and BCP+shdecorin rats: BCP rats treated with the decorin-targeting recombinant RNAi lentivirus. Values represent the mean \pm standard error of the mean (SEM), $n = 4$. * $p < 0.05$ compared with the sham group; # $p < 0.05$ compared with the BCP group. (d) Changes in PWT of the ipsilateral paw in the sham, BCP, BCP+shctrl, and BCP+shdecorin groups. Carcinoma implantation decreased the PWT of the ipsilateral paw of the rat, and shdecorin significantly reversed the reduction in PWT compared with the BCP rats. PWT: paw withdrawal threshold. Values represent the mean \pm SEM, $n = 8$. * $p < 0.05$ compared with the sham group; # $p < 0.05$ compared with the BCP group. BCP: bone cancer pain; PWT: paw withdrawal threshold.

Decorin promoted the phosphorylation level of GluR1 at serine 831 sites in the BCP rats

To examine the physiological effects of decorin on synaptic plasticity, We costained decorin in the spinal cord with synaptic markers and found that decorin was colocalized with vesicle protein synapsin I (a presynaptic marker) and PSD95 (an excitatory postsynaptic marker) in the superficial laminae of the dorsal horn (Figure 2(a)), which suggested that decorin plays a role in synaptic regulation. Western blot analysis (Figure 2 (b)) showed that the level of GluR1 in BCP rats did not change obviously as compared with the sham group ($p > 0.05$), while the phosphorylated GluR1 at serine 831 (pGluR1-ser831) was increased markedly in the

BCP group than in the sham group ($p < 0.05$). Treatment with shdecorin significantly decreased the expression of pGluR1-ser831 in the BCP+shdecorin group compared with the BCP group; however, the knockdown of decorin had no effect on the level of GluR1. The results suggested that the upregulation of pGluR1-ser831 at the spinal cord might promote the development of BCP, and decorin has the ability to regulate the phosphorylation of GluR1 at serine 831.

Our previous study demonstrated that sema3a is decreased in BCP rats and that the downregulation of sema3a in the spinal dorsal horn promotes the development of BCP by decreasing the phosphorylation level of cofilin (unpublished data). Either the recombinant lentivirus overexpressing sema3a (sema-LV) or the control

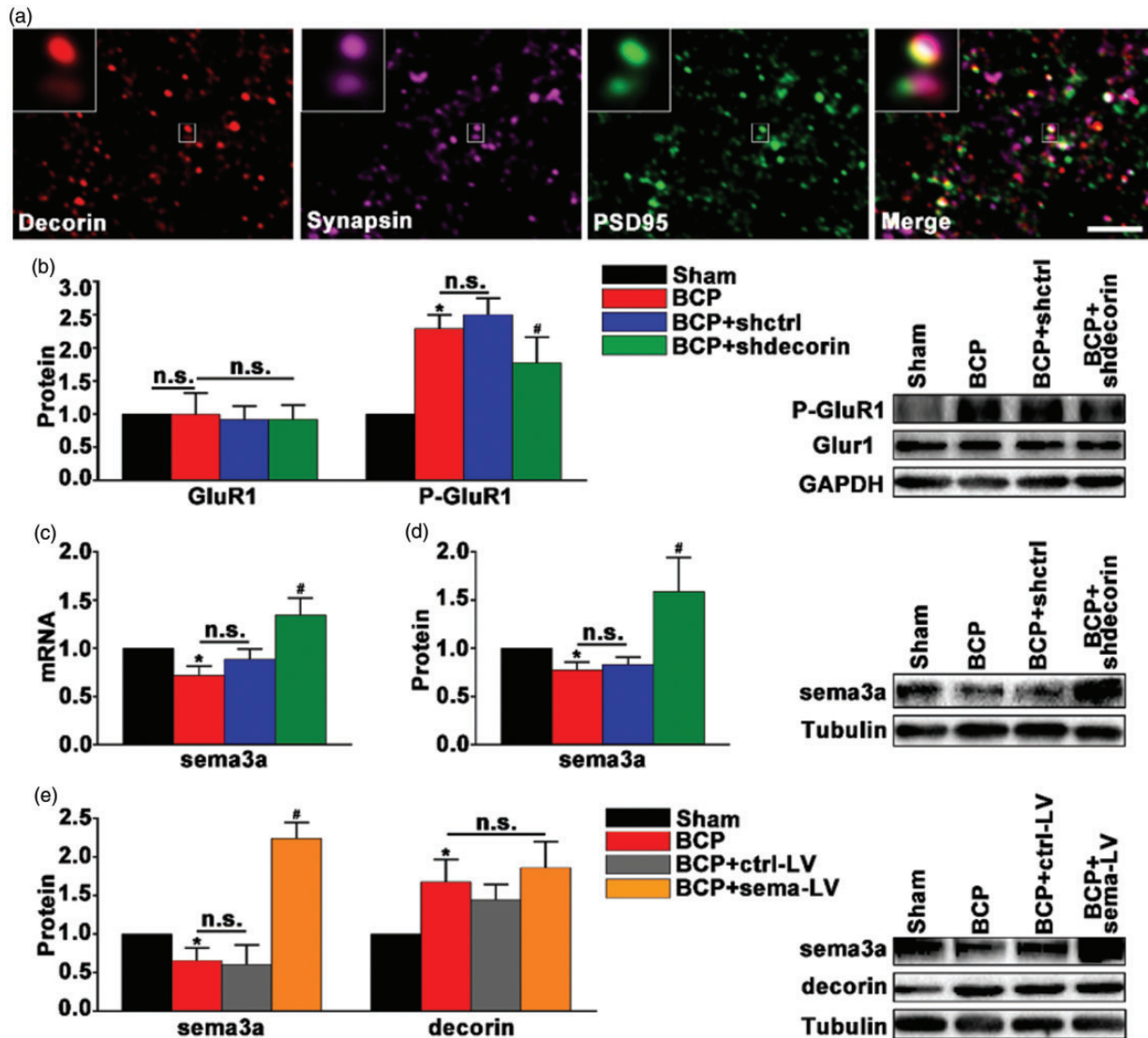


Figure 2. Decorin promoted the phosphorylation level of GluR1 at serine 831 in BCP rats. (a) Representative triple staining images of decorin (red), presynaptic marker of vesicle protein synapsin I (rose red), and excitatory postsynaptic marker PSD95 (green) in the superficial laminae of the spinal dorsal horn of the rats. Scale bar: 4 μm . (b) Western blot analysis of GluR1 and pGluR1 in the sham, BCP, BCP+shctrl, and BCP+shdecorin groups 21-day postsurgery. pGluR1: phosphorylation of GluR1 at the site of serine 831. Values represent the mean \pm standard error of the mean (SEM), $n = 4$. * $p < 0.05$ compared with the sham group; # $p < 0.05$ compared with the BCP group, n.s. indicates not significant. (c and d) Decorin negatively regulated sema3a in carcinoma-implanted rats. The effect of decorin on sema3a was confirmed by real-time polymerase chain reaction and western blot analysis in the four groups 21-day postsurgery. Values represent the mean \pm SEM, $n = 4$. * $p < 0.05$ compared with the sham group; # $p < 0.05$ compared with the BCP group. (e) Sema3a had no effect on decorin in the carcinoma-implanted rats. The effect of sema3a on decorin was confirmed by western blot analysis in the sham, BCP, BCP+ctrl-LV, and BCP+sema-LV rats 21-day postsurgery. BCP+ctrl-LV rats: BCP rats treated with the control lentivirus and BCP+sema-LV rats: BCP rats treated with the recombinant lentivirus overexpressing sema3a. Values represent the mean \pm SEM, $n = 4$. * $p < 0.05$ compared with the sham group, # $p < 0.05$ compared with the BCP group, n.s. indicates not significant ($p > 0.05$). BCP: bone cancer pain; PSD95: postsynaptic density protein 95; GAPDH: glyceraldehyde 3-phosphate dehydrogenase.

lentivirus (ctrl-LV) was microinjected into the ipsilateral dorsal horn of the BCP rats to study the relationship between decorin and sema3a. Real-time PCR and western blot analysis showed that sema3a expression was significantly higher in the BCP+shdecorin group than in the BCP group (Figure 2(c) and (d)). Treatment

with sema-LV remarkably improved the expression of sema3a in the BCP+sema-LV group, which showed that the lentivirus worked well. However, the level of decorin remained unchanged in the BCP+sema-LV group compared with that in the BCP group (Figure 2(e)). That is to say, the knockdown of

decorin could significantly decrease the reduction in sema3a expression in the spinal cord, while sema3a had no effect on the expression level of decorin. Together, these results suggest that decorin negatively regulates sema3a in BCP rats.

Decorin knockdown impaired the excitatory synaptogenesis and the insertion of pGluR1-ser831 into the excitatory postsynaptic membranes in vitro

To further examine the role of decorin in synaptic activity, we evaluated the effect of decorin on cultured cortical neurons in vitro. The neurons were first infected at DIV 3 with shdecorin or shctrl and fixed at DIV 12 to investigate the effect of decorin knockdown on the formation of excitatory synapses. The synapse formations were assayed by immunostaining for Bassoon (presynaptic active zone) and postsynaptic PSD95, whose colocalizations were considered structural excitatory synapses. The staining signals for the colocalization of Bassoon and PSD95 were significantly lower in the shdecorin group than in the shctrl group (10.8 ± 0.50 for shctrl, 8.3 ± 0.51 for shdecorin, $p < 0.01$; Figure 3(a) and (b)), and the signals for presynaptic Bassoon along the dendrites were markedly reduced in the shdecorin group (15.9 ± 0.73 for shctrl, 12.1 ± 0.76 for shdecorin, $p < 0.01$), in contrast, postsynaptic PSD95 remained unchanged in both groups (11.9 ± 0.49 for shctrl, 10.6 ± 0.41 for shdecorin, $p > 0.05$). These results suggested that decorin has an ability to promote the presynaptic differentiation and synaptogenesis of excitatory synapses in neurons. We next detected whether decorin is capable of regulating AMPARs in postsynaptic levels in vitro. After staining the transfected cortical neurons with antibodies against GluR1 and PSD95, we found that the fluorescence signals for GluR1 and the colocalization of GluR1 and PSD95 remained unchanged between the shctrl and shdecorin group (GluR1: 12.1 ± 0.54 for shctrl, 11.1 ± 0.39 for shdecorin, $p > 0.05$; colocalization: 8.7 ± 0.37 for shctrl, 9.4 ± 0.39 for shdecorin, $p > 0.05$; Figure 3(c) and (d)). Next, we examined the effect of decorin on the phosphorylation of GluR1. Interestingly, the results showed that the signals for pGluR1-ser831 were markedly lower in the shdecorin group than in the shctrl group and that the colocalization between pGluR1-ser831 and PSD95 was significantly reduced in the shdecorin group (pGluR1-ser831: 12.7 ± 0.51 for shctrl, 7.5 ± 0.39 for shdecorin, $p < 0.01$; colocalization: 10.1 ± 0.46 for shctrl, 6.4 ± 0.40 for shdecorin, $p < 0.01$; Figure 3(e) and (f)). These results suggested that decorin promotes the phosphorylation of synaptic GluR1 at Ser831 sites and clustering in postsynaptic activation zone.

Discussion

Several lines of evidence have showed that the ECM molecules participated in the process of pain regulation, and study demonstrated that the structural and biochemical plasticity in the hippocampal ECM are linked to the hyperalgesia in the chronic pain.²⁶ And the thrombospondin-4 participated in the development of the neuropathic pain by promoting the excitatory synaptogenesis.²⁷ Decorin, one of the most abundant matrix proteins of the ECM, is expressed by neurons, astrocytes, and Schwann cells in the peripheral and central nervous systems.²⁸ The present study was performed to determine the effect of decorin on the development of the BCP. In the study, we found that decorin was expressed in the gray matter of the spinal cord and that the expression was significantly increased in the spinal cord of the BCP rats, especially in the spinal dorsal horn. In addition, compared with rats from the sham group, cancer-bearing rats developed prominent pain from the seventh day. Interestingly, knockdown of decorin expression in the dorsal horn by shdecorin increased the PWT of cancer-bearing rats compared to that of rats from the sham group on the same day. These results suggested that decorin participates in the induction and maintenance of BCP.

The immunofluorescence in the spinal cord showed that decorin was colocalized with the excitatory pre- and postsynaptic markers, which indicated the role of decorin in the excitatory synaptic regulation. Therefore, in vitro experiments were designed to further detect the role of decorin in the synaptic regulation. Presynaptic activation zones are specialized regions of the presynaptic membrane where synaptic vesicles dock and fuse. Bassoon is an important presynaptic cytomatrix protein localized in the presynaptic activation zone and has been found to be recruited to the presynaptic bouton at the initial phase of synaptogenesis to promote synaptic targeting;²⁹ therefore, it is sufficient to facilitate the formation of neurotransmitter vesicles³⁰ and define the active zone as the site of neurotransmitter release in presynaptic boutons.³¹ In our present study, decorin knockdown decreased the density of bassoon in presynaptic membranes and decreased the number of excitatory synapses in neurons. That is to say, decorin had the ability to induce the formation of excitatory synapses, which might be mediated by promoting synaptic targeting in presynaptic levels. Our previous study²³ have demonstrated that excitatory synaptogenesis in the spinal dorsal horn induces central sensitization and contributes to BCP. Then, we conclude that decorin-mediated excitatory synaptogenesis might contribute to the development of the BCP.

The increased expression of the AMPAR in superficial dorsal horn contributes to central sensitization and

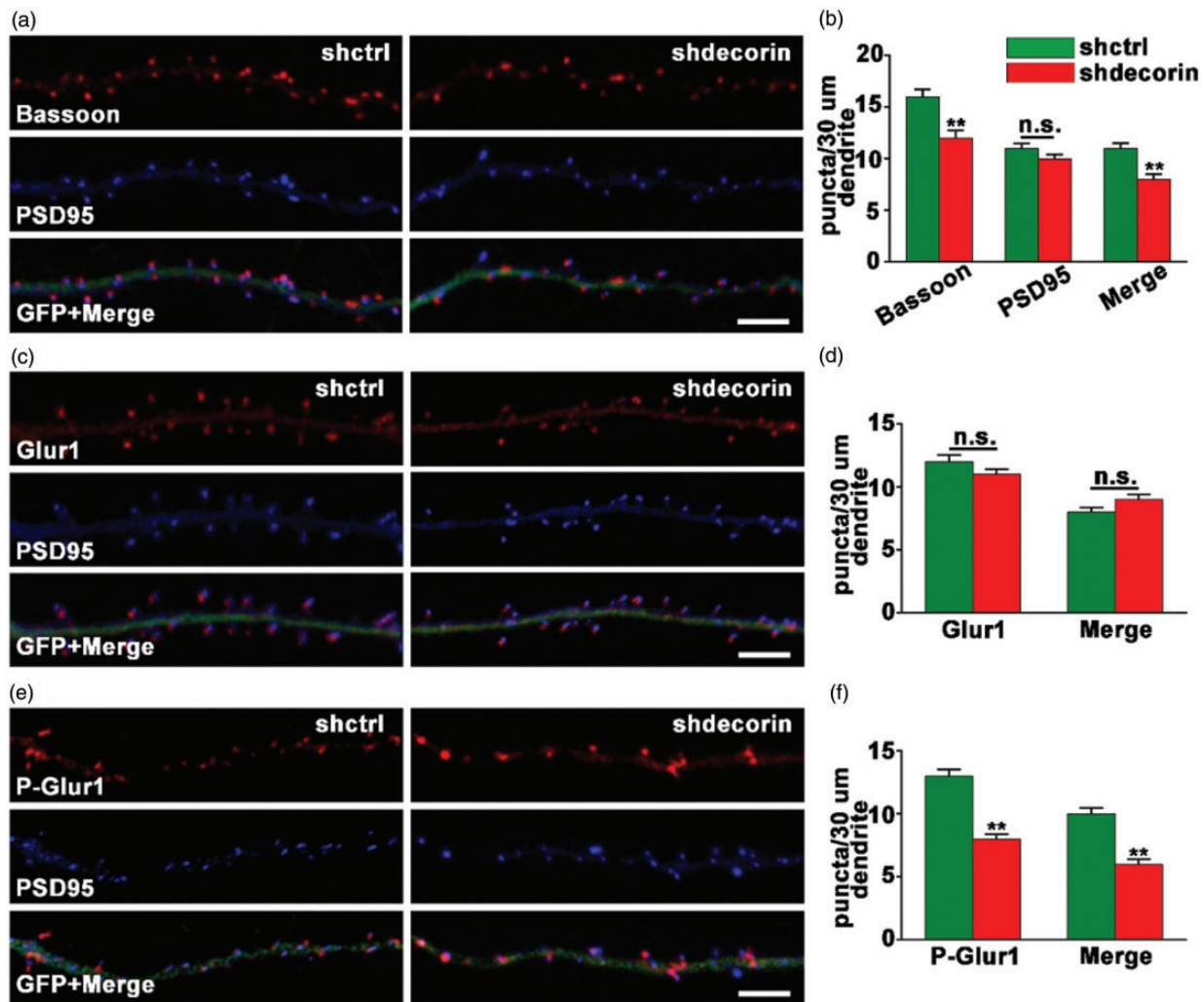


Figure 3. Decorin knockdown impaired the excitatory synaptogenesis and the insertion of pGluR1-ser831 into the excitatory postsynaptic membranes in vitro. Neurons were infected with lentivirus at DIV 3, and the immunofluorescence assay was performed at DIV 12: (a) Immunocytochemistry of dendrites from neurons in the shctrl and shdecorin groups at DIV 12 colabeled with antibodies against Bassoon (red) and PSD95 (blue) to visualize pre- and postsynaptic levels. Scale bar: 5 μ m; (b) Quantification of Bassoon, PSD95 and colocalization puncta in B per 30 μ m dendrite length. Values represent the mean \pm SEM, n = 30 in three independent experiments. **P < 0.01 compared with the shctrl group; n.s. indicates not significant (P > 0.05); (c) Immunofluorescence images of dendrites in DIV 12 neurons from the shctrl and shdecorin groups colabeled with antibodies against GluR1 (red) and PSD95 (blue). Scale bar: 5 μ m; (d) Quantification of GluR1 and colocalization puncta in B per 30 μ m dendrite length. Values represent the mean \pm SEM, n = 30 in three independent experiments. n.s. indicates not significant (P > 0.05); (e) Representative images of dendrites in DIV12 neurons from the shctrl and shdecorin groups colabeled with antibodies against GluR1 (red) and PSD95 (blue). Scale bar: 5 μ m and (f) Quantification of GluR1 and colocalization puncta in D per 30 μ m dendrite. Values represent the mean \pm SEM, n = 25 in three independent experiments. **P < 0.01 compared with the shctrl group.

heightened pain sensitivity, and AMPAR phosphorylation could lead to postsynaptic hyperexcitability during central sensitization.³² GluR1, an important subunit of the AMPARs, is abundantly distributed in laminae I and II of the spinal dorsal horn, which is the initial processing site for signals directly related to the transmission and modulation of pain.³³ Li³⁴ found that the increased phosphorylation of GluR1 at ser831 and ser845 on the ipsilateral side of the spinal dorsal horn in rats is induced

by plantar surface injection of capsaicin contributes to central sensitization. In addition, pGluR1-ser831 participated in the induction of complete Freund's adjuvant (CFA)-produced inflammatory pain but not neuropathic pain.³³ However, the roles of GluR1 and pGluR1 in BCP were not clarified.

In the present study, it was found that the level of pGluR1-ser831 was markedly increased in the spinal cord of the BCP rats. In addition, knocking down the

expression of decorin in the spinal dorsal horn prevented the increase in pGluR1-ser831 expression by BCP. While the level of GluR1 remained unchanged in the BCP rats, decorin knockdown did not change the level of GluR1 in BCP rats. In addition, in cultured neurons, decorin knockdown decreased the level of pGluR1-ser831 and the colocalization between pGluR1-ser831 and PSD95 in postsynaptic membranes but had no effect on the expression of GluR1, consistent with the *in vivo* results. Phosphorylation on ser831 of GluR1 may enhance synaptic transmission efficiency by lowering the threshold for AMPAR trafficking to synapses^{35,36} and by promoting AMPAR delivery to synaptic membranes.³⁷ Our results suggested that upregulation of decorin might promote the trafficking and insertion of pGluR1-ser831 to postsynaptic membranes in the dorsal horn of BCP rats.

Our previous study has demonstrated that sema3a is significantly decreased in the BCP rats and promotes the development of the BCP through regulating phosphorylation of cofilin 1 in the dorsal horn. In the present study, we found that the reduction in sema3a expression was markedly prevented by decorin knockdown in the spinal cord. In contrast, overexpression of sema3a in the spinal cord had no effect on the expression level of decorin. Taken together, these results indicated that decorin is a negative upstream regulator of sema3a in the BCP. This result was coincident with Minor²¹ study, they demonstrated that decorin could reduce the messenger RNA and protein levels of sema3a in injured central nervous system. Cofilin 1 is the important regulator of actin cytoskeleton, and previous studies have reported that cofilin 1 has essential functions in neuriteogenesis, neurite elongation, dendritic spine formation, and synaptic plasticity.^{38,39} Therefore, we suggest that the ability of decorin to regulate synaptogenesis might be mediated by regulating the sema3a/cofilin 1 pathway.

However, there are still some limitations in our study. Although we have observed a negative regulation between decorin and sema3a in the BCP, the potential regulatory mechanism is unclear. And in our experiment, the immunofluorescence analysis showed that the expression of decorin appeared to be increased in the ventral horn of BCP rats, then the further studies are needed to clarify the role of decorin in the ventral horn of the BCP. In addition, as the survival rate of spinal cord neurons is low *in vitro*, and the synaptic connections are fewer between spinal cord neurons, the cortical neurons instead of spinal neurons were used to detect the biological effects of decorin *in vitro*; therefore, the true potential of decorin to promote the development of cancer pain might need to be tested in transgenic mice.

Taken together, the results of the present study showed that the expression level of decorin was significantly upregulated in the spinal dorsal horn of rats with cancer pain induced by carcinoma implantation into the

tibial plateau; moreover, knockdown of decorin expression in the spinal dorsal horn could attenuate the mechanical allodynia in the BCP rats and was likely mediated by regulating the sema3a/cofilin 1 pathway to inhibit the excitatory synaptogenesis in the spinal dorsal horn, thereby reducing the clustering and insertion of pGluR1-ser831 to postsynaptic membranes. These findings suggest that decorin might be a potential therapeutic target for alleviating BCP. Moreover, our real-time quantitative PCR analysis also showed that the mRNA of decorin was significantly upregulated in sciatic nerve injury (SNI) rats (data not shown), we suggest that decorin might regulate the pain by general mechanism.

Authors' Contributions

Changbin Ke and Juying Liu conceived the project and designed the experiments. Huan Wang, Xiaohui Li, Xianqiao Xie, and Haiwen Zhao performed the experiments. Yan Gao, Yang Li, Xueqin Xu, and Xiaofei Zhang analyzed the data. Huan Wang wrote the paper under the guidance of Changbin Ke and Juying Liu.

Declaration of Conflicting Interests

The author(s) declared no potential conflicts of interest with respect to the research, authorship, and/or publication of this article.

Funding

The author(s) disclosed receipt of the following financial support for the research, authorship, and/or publication of this article: This study was supported by the Natural Science Foundation of Hubei Province of China (No. 2017CFB475) and the Shiyuan Bureau of Science and Technology (No. 17K71 and No. 17Y18).

ORCID iD

Huan Wang  <https://orcid.org/0000-0002-0287-4938>

References

1. Hua B, Gao Y, Kong X, Yang L, Hou W, Bao Y. New insights of nociceptor sensitization in bone cancer pain. *Expert Opin Ther Targets* 2015; 19: 227–243.
2. Sarah F, Anthony HD. Pain and nociception: mechanisms of cancer-induced bone pain. *J Clin Oncol* 2014; 32: 1647–1654.
3. Kuner R, Flor H. Structural plasticity and reorganisation in chronic pain. *Nat Rev Neurosci* 2017; 18: 20–30.
4. Mantyh P. Bone cancer pain: causes, consequences, and therapeutic opportunities. *Pain* 2013; 154: S54–S62.
5. Zhou Y-Q, Liu Z, Liu H-Q, Liu D-Q, Chen S-P, Ye D-W, Tian Y-K. Targeting glia for bone cancer pain. *Expert Opin Ther Targets* 2016; 20: 1365–1374.
6. Kawasaki Y, Zhang L, Cheng JK, Ji RR. Cytokine mechanisms of central sensitization: distinct and overlapping role of interleukin-1, interleukin-6, and tumor necrosis

- factor- α in regulating synaptic and neuronal activity in the superficial spinal cord. *J Neurosci* 2008; 28: 5189–5194.
7. Greger IH, Watson JF, Cull-Candy SG. Structural and functional architecture of AMPA-type glutamate receptors and their auxiliary proteins. *Neuron* 2017; 94: 713–730.
 8. Martineau M, Guzman RE, Fahlke C, Klingauf J. VGLUT1 functions as a glutamate/proton exchanger with chloride channel activity in hippocampal glutamatergic synapses. *Nat Commun* 2017; 8: 2279.
 9. Twomey EC, Yelshanskaya MV, Grassucci RA, Frank J, Sobolevsky AI. Channel opening and gating mechanism in AMPA-subtype glutamate receptors. *Nature* 2017; 549: 60–65.
 10. Dai W-L, Yan B, Jiang N, Wu J-J, Liu X-F, Liu J-H, Yu B-Y. Simultaneous inhibition of NMDA and mGlu1/5 receptors by levo-corydalmine in rat spinal cord attenuates bone cancer pain. *Int J Cancer* 2017; 141: 805–815.
 11. Ricciardelli C, Lokman NA, Sabit I, Gunasegaran K, Bonner WM, Pyragius CE, Macpherson AM, Oehler MK. Novel ex vivo ovarian cancer tissue explant assay for prediction of chemosensitivity and response to novel therapeutics. *Cancer Lett* 2018; 421: 51–58.
 12. Zhou L, Jing J, Wang H, Wu X-J, Lu Z-F. Decorin promotes proliferation and migration of ORS keratinocytes and maintains hair anagen in mice. *Exp Dermatol* 2018; 27:1237–1244.
 13. Dityatev A, Schachner M. Extracellular matrix molecules and synaptic plasticity. *Nat Rev Neurosci* 2003; 4: 456–468.
 14. Levy AD, Omar MH, Koleske AJ. Extracellular matrix control of dendritic spine and synapse structure and plasticity in adulthood. *Front Neuroanat* 2014; 8: 116–111.
 15. Hellwig S, Hack I, Kowalski J, Brunne B, Jarowij J, Unger A, Bock HH, Junghans D, Frotscher M. Role for Reelin in Neurotransmitter Release. *J Neurosci* 2011; 31: 2352–2360.
 16. Gronau T, Krüger K, Prein C, Aszodi A, Gronau I, Iozzo RV, Mooren FC, Clausen-Schaumann H, Bertrand J, Pap T, Bruckner P, Dreier R. Forced exercise-induced osteoarthritis is attenuated in mice lacking the small leucine-rich proteoglycan decorin. *Ann Rheum Dis* 2017; 76: 442–449.
 17. Horváth Z, Kovalszky I, Fullár A, Kiss K, Schaff Z, Iozzo RV, Baghy K. Decorin deficiency promotes hepatic carcinogenesis. *Matrix Biol* 2014; 35: 194–205.
 18. Esmaili M, Berry M, Logan A, Ahmed Z. Decorin treatment of spinal cord injury. *Neural Regen Res* 2014; 9: 1653–1656.
 19. Minor K, Tang X, Kahrilas G, Archibald SJ, Davies JE, Davies SJ. Decorin promotes robust axon growth on inhibitory CSPGs and myelin via a direct effect on neurons. *Neurobiol Dis* 2008; 32: 88–95.
 20. Pasterkamp RJ, Giger RJ. Semaphorin function in neural plasticity and disease. *Curr Opin Neurobiol* 2009; 19: 263–274.
 21. Minor KH, Bournat JC, Toscano N, Giger RJ, Davies S. Decorin, erythroblastic leukaemia viral oncogene homologue B4 and signal transducer and activator of transcription 3 regulation of semaphorin 3A in central nervous system scar tissue. *Brain* 2011; 134: 1140–1155.
 22. Zimmermann M. Ethical guidelines for investigations of experimental pain in conscious animals. *Pain* 1983; 16: 109–110.
 23. Ke C, Li C, Huang X, Cao F, Shi D, He W, Bu H, Gao F, Cai T, Hinton AO, Tian Y. Protocadherin20 promotes excitatory synaptogenesis in dorsal horn and contributes to bone cancer pain. *Neuropharmacology* 2013; 75: 181–190.
 24. Peviani M, Kurosaki M, Terao M, Lidonnici D, Gensano F, Battaglia E, Tortarolo M, Piva R, Bendotti C. Lentiviral vectors carrying enhancer elements of Hb9 promoter drive selective transgene expression in mouse spinal cord motor neurons. *J Neurosci Methods* 2012; 205: 139–147.
 25. Laguesse S, Morisot N, Shin JH, Liu F, Adrover MF, Sakhai SA, Lopez MF, Phamluong K, Griffin WC, Becker HC, Bender KJ, Alvarez VA, Ron D. Prosapip1-dependent synaptic adaptations in the nucleus accumbens drive alcohol intake, seeking, and reward. *Neuron* 2017; 96: 145–159.e8.
 26. Tajerian M, Hung V, Nguyen H, Lee G, Joubert L-M, Malkovskiy AV, Zou B, Xie S, Huang T-T, Clark JD. The hippocampal extracellular matrix regulates pain and memory after injury. *Mol Psychiatry* 2018; 23: 2302–2313.
 27. Park JF, Yu YP, Gong N, Trinh VN, Luo ZD. The EGF-LIKE domain of thrombospondin-4 is a key determinant in the development of pain states due to increased excitatory synaptogenesis. *J Biol Chem* 2018; 293: 16453–16463.
 28. Hanemann CO, Kuhn G, Lie A, Gillen C, Bosse F, Spreyer P, Müller HW. Expression of decorin mRNA in the nervous system of rat. *J Histochem Cytochem* 1993; 41: 1383–1391.
 29. Dresbach T, Hempelmann A, Spilker C, Tom Dieck S, Altmann WD, Zuschratter W, Garner CC, Gundelfinger ED. Functional regions of the presynaptic cytomatrix protein bassoon: significance for synaptic targeting and cytomatrix anchoring. *Mol Cell Neurosci* 2003; 23: 279–291.
 30. Maas C, Torres VI, Altmann WD, Leal-Ortiz S, Wagh D, Terry-Lorenzo RT, Fejtova A, Gundelfinger ED, Ziv NE, Garner CC. Formation of Golgi-derived active zone precursor vesicles. *J Neurosci* 2012; 32: 11095–11108.
 31. Zhai R, Olias G, Chung WJ, Lester RAJ, Tom Dieck S, Langnaese K, Kreutz MR, Kindler S, Gundelfinger ED, Garner CC. Temporal appearance of the presynaptic cytomatrix protein bassoon during synaptogenesis. *Mol Cell Neurosci* 2000; 15: 417–428.
 32. Latremoliere A, Woolf CJ. Central sensitization: a generator of pain hypersensitivity by central neural plasticity. *J Pain* 2009; 10: 895–926.
 33. Lu Y, Sun Y-N, Wu X, Sun Q, Liu F-Y, Xing G-G, Wan Y. Role of α -amino-3-hydroxy-5-methyl-4-isoxazolepropionate (AMPA) receptor subunit GluR1 in spinal dorsal horn in inflammatory nociception and neuropathic nociception in rat. *Brain Res* 2008; 1200: 19–26.
 34. Li F, Wu J, Lin Q, Willis WD. Protein kinases regulate the phosphorylation of the GluR1 subunit of AMPA receptors of spinal cord in rats following noxious stimulation. *Mol Brain Res* 2003; 118: 160–165.
 35. Lu W, Roche KW. Posttranslational regulation of AMPA receptor trafficking and function. *Curr Opin Neurobiol* 2012; 22: 470–479.

36. Kristensen AS, Jenkins MA, Banke TG, Schousboe A, Makino Y, Johnson RC, Haganir R, Traynelis SF. Mechanism of Ca²⁺/calmodulin-dependent kinase II regulation of AMPA receptor gating. *Nat Neurosci* 2011; 14: 727–735.
37. Robison AJ. Emerging role of CaMKII in neuropsychiatric disease. *Trends Neurosci* 2014; 37: 653–662.
38. Shaw AE, Bamberg JR. Peptide regulation of cofilin activity in the CNS: a novel therapeutic approach for treatment of multiple neurological disorders. *Pharmacol Ther* 2017; 175: 17–27.
39. Cingolani LA, Goda Y. Actin in action: the interplay between the actin cytoskeleton and synaptic efficacy. *Nat Rev Neurosci* 2008; 9: 344–356.